BioMACROMOLECULES

ARTICLE

pubs.acs.org/Biomac

"Nanocellulose" As a Single Nanofiber Prepared from Pellicle Secreted by *Gluconacetobacter xylinus* Using Aqueous Counter Collision

Ryota Kose, Ikue Mitani, Wakako Kasai, and Tetsuo Kondo*

Graduate School of Bioresource and Bioenvironmental Sciences, Kyushu University, 6-10-1, Hakozaki, Higashi-ku, Fukuoka, 812-8581, Japan

ABSTRACT: This study attempted to prepare a single cellulose nanofiber, "nanocellulose", dispersed in water from 3D networks of nanofibers in microbial cellulose pellicle using aqueous counter collision (ACC), which allows biobased materials to be down-sized into nano-objects only using water jets without chemical modification. The nanocellulose thus prepared exhibited unique morphological properties. In particular, the width of the nanocellulose, which could be controlled as desired on nanoscales, was smaller than that of just secreted cellulose nanofiber, resulting in larger specific surface areas. Moreover, ACC treatment transformed cellulose I_α crystalline phase into cellulose I_β phase with the crystallinity kept >70%. In this way, ACC method depending on the treatment condition could provide the desired fiber width at the nanoscale and the different ratios of the two crystalline allomorphs between cellulose I_α versus I_β, which thus opens further pathways into versatile applications as biodegradable single nanofibers.

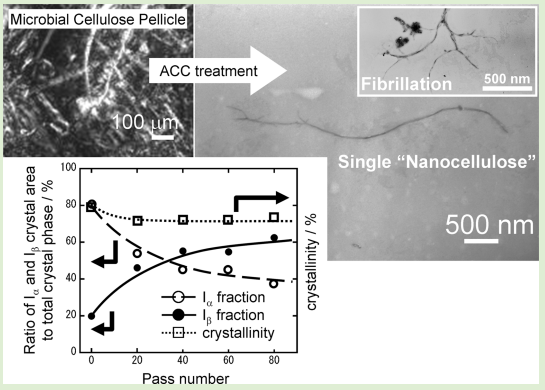

INTRODUCTION

Gluconacetobacter xylinus (*Acetobacter xylinum*) secretes a cellulose nanofiber that comprises a microfibril having ca. 3.5 nm in width. The microfibrils are supposed to assemble by interfacial interactions including hydrogen bonding and van der Waals force between the component molecules, resulting in forming a ribbon-like cellulose nanofiber with ca. 50 nm in width and 10 nm in thickness, respectively.[1] The nanofibers are then engaged in a 3D network to provide with a gel-like membrane called pellicle, because of random movements accompanied with fiber secretion of the bacteria in a culture medium. To date, the pellicle has been extensively studied as a most promising biobased material having versatile properties, for example, biocompatibility,[2] high water retaining capacity, high crystallinity, and high mechanical strength.[3] Further investigations have also been performed to open wider application fields of tissue engineering,[4,5] electronic device,[6] emulsifiers,[7] nanocomposite,[8] and so on.[9,10] Most applications above are induced by the unique 3D network structure constructed with cellulose nanofibers to be employed as a key for the function.

This study does not focus on the network, but the single nanofiber from the viewpoint of the width on the nanoscale and the microsized length longer than other cellulose fibers,[11] which is expected to exhibit a high adsorptivity enhanced by the large specific surface areas. Besides the sizes, the crystallinity of the microbial cellulose fiber is remarkably high by >90%.[12] This could be responsible for rigidity and low expansion of the single nanofiber, which is independent of the surrounding temperature. Moreover, the microbial fiber is made up by a composite of the two crystalline phases, cellulose I_α and I_β, with the ratio of I_α/I_β = 65/35.[13,14] The cellulose I_α phase has been reported to locate as surroundings of a core domain of cellulose I_β phase in a single nanofiber.[14]

Recently, the authors proposed an aqueous counter collision (ACC)[15,16] method to allow biobased materials to be downsized into nano-objects only using water jets as the medium without chemical modification of the molecules including depolymerization. In this ACC system, an aqueous suspension containing microsized samples, which are predivided into a pair of facing nozzles, are supposed to collide with each other at a high rate, resulting in wet and rapid pulverization of the samples into nanoscaled objects dispersed in water. The obtained materials are more downsized by repeating the collision and increasing in the ejecting pressure.

In this article, ACC method has been employed for microbial cellulose pellicle produced by *Gluconacetobacter xylinus* to provide with the single cellulose nanofibers, "nanocellulose", having novel morphological properties including alteration of crystalline phases. The nanocellulose is likely to exhibit some specific surface properties as well as morphological characteristics as a single nanofiber.

EXPERIMENTAL SECTION

Materials. Components of the SH culture medium[17] were as follows: D-glucose, citric acid, and sodium hydroxide with a culture grade, which were purchased from Wako Chemicals. Di-sodium hydrogenphosphate heptahydrate with a culture grade was purchased from Nacalai Tesque. Yeast extracts and peptone were provided from Bectom,

Received: November 11, 2010
Revised: January 15, 2011
Published: February 11, 2011

Dickinson and Company. Deionized water was used for ACC treatment of cellulose samples.

Preparation of Cellulose Nanofiber, "Nanocellulose". Following inoculated into the SH culture medium in a sterilized plastic container, *Gluconacetobacter xylinus* (= *Acetobacter xylinum*: ATCC-53582) was cultured statically at 30 °C to yield a gel-like membrane having a 3D network structure of the secreted cellulose nanofibers, termed microbial cellulose pellicle. After 2 weeks of incubation, the pellicle with ca. 1 cm in thickness was established, covering the top of the culture medium. The pellicle was picked up before being washed with 0.1% aqueous NaOH solution at 80 °C for 4 h and successively with water over 3 days to remove protein, bacterial cells, and other residues. The purified pellicle was cut into ca. 1 cm^3 cubes by scissors prior to immersion in deionized water. Crystallinity of cellulose in this cube exhibited 84%. The mixture containing ≤0.4% (w/w) cellulose fibers in water was pretreated using a homogenizer, Physcotron NS-51, (Microtec) for <5 min at 20 000 rpm to provide with pieces of the pellicle having ca. 180 μm in width. After the homogenization, the crystallinity was reduced from 84 to 79%. The suspended mixture was then provided for ACC treatment[15,16] using ACC system (Sugino, Japan) under 200 MPa of the ejecting pressure with 10-, 20-, 30-, 40-, 60-, and 80-cycle repetition times (= pass), resulting in the dispersion of single-cellulose nanofibers in water. We term this single nanofiber as "nanocellulose" in the following section.

FTIR Measurement. After the suspension obtained above was dropped on a silicon substrate and air-dried to remove water at ≤50 °C, it was completely dried under vacuum at 60 °C for preparation of film specimens. FTIR spectra for the film samples were measured using a JASCO FTIR-620 (Japan Spectroscopy) spectrophotometer. The condition for the FTIR measurements was as follows: 32 scans with a 2 cm^{-1} resolution equipped with a TGS detector, and the wavenumber region investigated ranged from 4000 to 400 cm^{-1}. They were normalized using the band at 1162 cm^{-1} corresponding to the C−O stretching mode to compare the individual spectra, except for the polarized ones.

Wide-Angle X-ray Diffraction (WAXD). The aqueous suspension containing nanofibers was frozen in a freezer at −20 °C and vacuum-dried. WAXD measurements of the dried sample were carried out using a Rigaku Rint-2500F X-ray generator (Rigaku) equipped with a pinhole collimator having 1 mm in diameter. The nickel-filtered Cu Kα radiation was produced at 40 kV and 200 mA. The sample was measured by a transmission mode with a scanning speed of 0.05°/min and in the 5−35° diffraction angle range. To determine the crystallinity, the diffraction curves were deconvoluted by curve fitting analysis using Gaussian functions.[18,19] The resulting diffraction patterns exhibited four typical diffraction peaks assigned to the cellulose crystal lattice, and one broad peak assigned to amorphous regions. Crystallinity was calculated by the following expression

$$\text{crystallinity}/\% = (\text{total areas of four typical diffraction peaks}/\text{total areas of crystalline and amorphous peaks}) \times 100$$

CP/MAS ^{13}C NMR. The ^{13}C cross-polarization/magic angle spinning (CP/MAS) NMR measurements of the same sample specimens for the WAXD described above were performed using a Chemagnetics CMX 300 spectrometer (Chemagnetics) operating at 300 MHz for ^{1}H and 75.6 MHz for ^{13}C, respectively. The repetition time was 3 s, and the cross-polarization (CP) contact time was 8 ms. The carbon signal (C−H) of adamantine was used as an external reference to determine the chemical shifts. To determine the I_α fraction in the whole cellulose crystalline phase, the characteristic ^{13}C NMR signals due to C1 carbons were deconvoluted by a Lorenzian curve fitting analysis.[20] The resulting spectra exhibited one line assigned to I_α crystal lattice and two lines assigned to I_β crystal lattice. The I_α fraction was calculated by the following expression

$$I_\alpha \text{ fraction}/\% = (\text{areas of one line assigned to } I_\alpha \text{ crystalline phase}/\text{total areas of three lines}) \times 100$$

Transmission Electron Microscopy (TEM). Observation by TEM was employed for measurements of both width and length of a single-cellulose nanofiber, "nanocellulose". Prior to observing the nanocellulose, 10 mL of ca. 0.04% (w/v) aqueous suspension was mixed with 10 mL of 0.4% (w/w) of poly(vinyl alcohol) (PVA) aqueous solution to avoid self-aggregation of the nanofibers. The mixture was stirred at 50 °C for 3 days before being diluted to 1/10 concentration by deionized water. Then, 1 mL of the suspension was added to 9 mL of 0.2% uranium acetate aqueous solution. The mixture was sonicated with an ultrasonic apparatus for 10 s, mounted on copper grids, and finally air-dried. Nanocellulose on the grid was observed using a JEM-1010 (JEOL) apparatus at 80 kV of the accelerating voltage. The negative films of the acquired images were scanned to be digitized for measurements of width and length in the individual nanocellulose.

Surface Area Measurements. An aqueous suspension containing nanofibers was poured in a test tube for measurements of the total surface areas of the fibers. The test tube was then quenched in N_2 liquid to freeze the aqueous suspension. Following freeze-drying, it was kept at 100 °C for 20 min to almost completely evaporate water bound to cellulose nanofibers. A surface area analyzer, Monosorb (Quantachrome Instruments), was used to measure N_2 sorption onto the cellulose nanofibers at 77 K. The surface areas were estimated from fitting of adsorption data to the Brunauer, Emmett and Teller equation.[21] The specific surface areas of the nanocellulose were obtained by dividing the surface areas with total weight of the nanofibers.

Viscosity Measurements. An intrinsic viscosity $[\eta]$ of a cellulose sample was measured in a copper ethylene diamine solution according to the previous method.[22,23] From the viscosity, a degree of polymerization was calculated according to the following equation between intrinsic viscosity and degree of polymerization

$$[\eta] = 1.67 \times DP^{0.71} \quad (DP \cong [\eta] \times 190)$$

where 1.67 and 0.71 are intrinsic for cellulose/copper ethylene diamine solution.

RESULTS AND DISCUSSION

Morphological Changes of Nanocellulose during ACC Treatment. The pellicle disintegrated in the size range of 1.2 ± 0.5 mm by a homogenizer was provided for ACC treatment with 30 repetition times (pass). Before the treatment, the network structure of fibers in the pellicle was visible by a polarized optical microscope (Figure 1a). After a few pass of the ACC treatment, nothing was any more observed using a polarized optical microscope (Figure 1b), but instead a fiber having nanosized width could be observed by TEM, as shown in Figure 1c. This indicates that ACC treatment rendered the network in the pellicle to be easily and rapidly liberated into single cellulose nanofibers, namely, nanocellulose. It is noted that a typical morphological change by repetition of ACC treatment was further fibrillation of the nanocellulose, as indicated by arrows in Figure 1c. The fibrillation exposes internal faces in nanocellulose onto the surface to increase the surface areas of nanocellulose. Table 1 lists specific surface areas of cellulose nanofibers obtained by the ACC treatments with 30 and 60 pass. Both specific surface areas were higher than those of microcrystalline cellulose,[24] microbial cellulose film,[25] and disintegrated pellicle

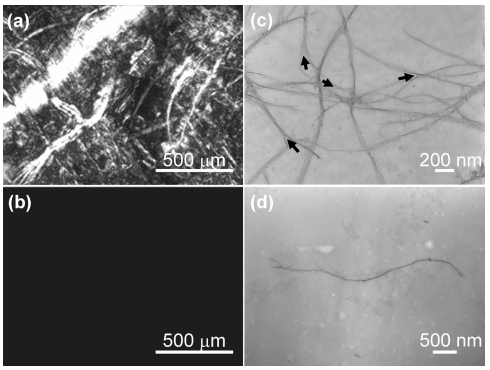

Figure 1. Optical microscopic images of cellulose pellicle (a) before and (b) after ACC treatment. (c) Transmission electron microscopic image of nanocellulose provided by ACC treatment with 30 Pass. An arrow indicates a knot of fibrillation in nanocellulose. (d) Transmission electron microscopic image of entire shape of a nanocellulose provided by ACC treatment with 40 Pass for measurement of width and length. The sample specimen did not contain PVA.

Table 1. Specific Surface Areas for Freeze-Dried Nanocellulose before and after ACC Treatment

	nanocellulose			MCC[a]	MC film[b]
pass number	0	30	60		
specific aspect area/$m^2 \cdot g^{-1}$	43.0	54.5	55.9	1.3	12.62

[a] MCC: microcrystalline cellulose (ref 19). [b] MC film: microbial cellulose film (ref 20).

without ACC treatment. It is, therefore, expected that nanocellulose obtained in this article has a fairly high adsorbability encouraged by the high specific surface areas.

Width and length of nanocellulose was hard to measure because of the self-aggregation on the grid during sample preparation for observation by TEM. Aggregation-free nanocellulose on the grid (Figure 1d) was, therefore, selectively employed for the measurements of width and length, respectively. Width of the nanocellulose was decreased with increasing in pass number in ACC treatment, as listed in Table 2. This also indicated that ACC treatment was rapidly capable to downsize further the initial nanofiber into nanocellulose having ca. 30 nm in width at 40 pass under 200 MPa as the ejecting pressure. Considering the reduction behavior in width accompanied with ACC treatment, the treatment at the same ejecting pressure could not provide a further significant effect on the downsizing process following 40 pass (Table 2). This means that once a synergetic effect induced by ACC treatment reached a certain level, additional liberation of the interfacial interaction did not occur any more. Suppose that the collision energy in the ACC treatment is at a certain magnitude; some weaker interfacial interaction in the individual secreted cellulose nanofibers could be cleaved by the treatment, but the stronger interfacial interaction would still remain. Namely, liberation of the interaction in the present case depends on whether the bonding energy is higher or smaller than the collision energy under 200 MPa as the ejecting pressure of water in ACC treatment. The energy is assumed to be at most 13.4 kJ/mol, which is more than that for weaker hydrogen bonds, the corresponding medium hydrogen bonds, or both.[16] The 13.4 kJ/mol was obtained by calculating the kinetic energy of the jetted water under 200 MPa as the ejecting pressure.[16]

Table 2. Width, Length, and Aspect Ratio of Nanocellulose Obtained by ACC Treatment at Each Pass Number under 200 MPa As the Ejecting Pressure

pass number	width/nm	length/μm	aspect ratio[a]
0	69 ± 35	23.9 ± 19.3	346
20	48 ± 34	$5.0 + 4.1$	102
40	33 ± 14	3.3 ± 2.0	101
60	34 ± 13	$3.8 + 1.9$	14
80	31 ± 11	3.1 ± 2.3	99

[a] Aspect ratio was calculated by division of the average length by the average width.

Therefore, the obtained nanocellulose having 30 nm in width was possibly engaged with a medium hydrogen bond having higher interaction energy than the collision energy. This indicates that the nanocellulose maintains a still assembly status of a microfibril having ca. 3.5 nm in width because the initially secreted cellulose nanofiber comprises a bundle of the individual microfibril assembled by interfacial interactions mainly including hydrogen bonding between the component molecules.[1,16,26]

The length of the nanocellulose was drastically shortened with ACC treatment in comparison with the starting material before the treatment (Table 2). Once it reached ca. 5.0 μm, the drastic change was ceased; thereafter, the length was kept within 5.0 ± 2 μm. Namely, the longitudinal length of nanocellulose decreased rapidly with increasing the pass number between 0 and 20 pass. Then, a gradual change in the length occurred after 20 pass to reach finally the value of the length of 3.1 ± 2.3 μm at 80 Pass. Here viscometric measurements for the homogenized nanofibers provided a value of 1.2 μm as the molecular chain length based on the average viscometric degree of polymerization (2400), which was shorter than the treated fiber length. Taking the high crystallinity of the fiber and the collision energy with less than the covalent bonding energy into account, ACC treatment could break the fiber in the space between ends of the molecular chains. The aspect ratios exhibited ca.100 constantly after >20 pass, as shown in Table 2. The constant value of ca. 100 as the aspect ratio might have some biologically structural meaning. In addition, the value was higher than 20 and 40 for cellulose nanocrystal/whisker reported in a previous paper.[27] Therefore, it is also expected that the nanocellulose has a significant effect for reinforcement as nanofiller in composites.

Moreover, as shown in Table 2, the average length and width of nanocellulose were saturated already at 20 Pass, whereas both of the standard deviations were further reduced with increasing in pass number. This indicates that the more repetition of ACC treatment allowed width and length of the nanocellulose to be more homogenously downsized into ca. 30 nm and 2 to 3 μm, respectively.

Crystalline Structure of Nanocellulose. It is well-known that a cellulose nanofiber secreted by the bacterium is made up by a composite of the two crystalline phases, cellulose I_α and I_β ($I_\alpha/I_\beta = 65/35$).[13,14] Figure 2 shows change of FTIR spectra for the ACC-treated pellicle depending on pass number. The entire spectra indicated that the crystalline structure in secreted cellulose nanofibers was made up with cellulose I.[28] Namely, ACC treatment did not transform it to other cellulose crystalline allomorphs,[15,16] for example, cellulose II. However, it was found that the ratio of cellulose I_α to total crystal phases in the nanocellulose decreased with increasing in pass number. In Figure 2, the two typical absorption bands at 3270 and 710 cm^{-1}

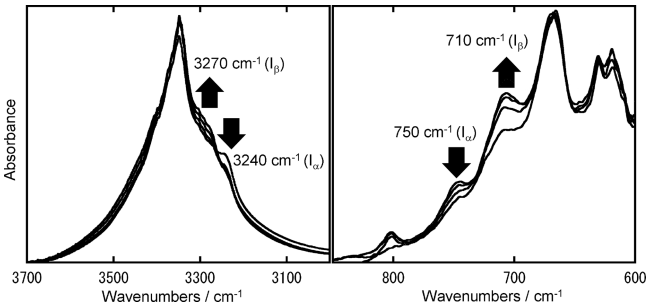

Figure 2. FTIR spectra showing the change of the ratio of cellulose I_α phase to cellulose I_β phase depending on pass number of 0, 10, 30, and 60, respectively. The wide arrows indicate tendency of changes at the characteristic bands depending on increase in Pass number from 0 to 60.

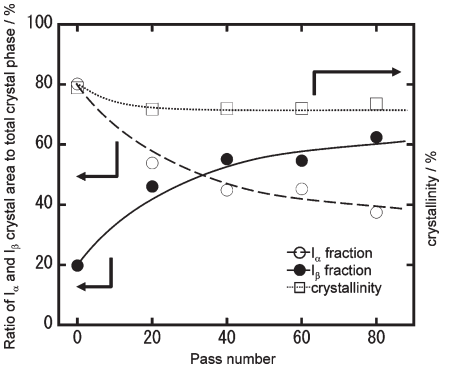

Figure 3. Dependence of Pass number on change of the ratio of cellulose I_α and I_β phase in nanocellulose measured by CP/MAS ^{13}C NMR together with the crystallinity measured by WAXD.

attributed to cellulose I_β phase increased, whereas those at 3250 and 750 cm^{-1} attributed to cellulose I_α phase decreased with increasing pass number.[29,30] To investigate quantitatively the ratios of cellulose I_α to the total crystalline phases, CP/MAS ^{13}C NMR spectroscopy was employed for the samples with systematically changing pass number. The crystallinity was also measured by X-ray diffraction. As shown in Figure 3, the ratio of cellulose I_α rapidly decreased from 80 to 45% in the range from 0 to 40 pass, followed by a slow decrease from 45 to 38% at 80 pass. In contrast, cellulose I_β content was increased from 20 to 55% in the range from 0 to 40 pass with a further slow increase from 55 until 62% at 80 pass. During the crystalline transformation behavior, the total crystallinity in nanocellulose was not significantly changed. Namely, it was saturated as ca. 70% until 80 pass. These behaviors may contain a two-fold phenomenon: (i) ACC treatment allowed cellulose I_α crystalline phase to be transformed into cellulose I_β, which was supported by the previous report that I_β phase was thermodynamically more stable than I_α phase.[20,31] (ii) The transformation from cellulose I_α to I_β occurred on the nanofiber surface. In other words, the shear stress due to the collision energy of water at a high speed in ACC treatment enhanced sliding of cellulose molecules in the cellulose I_α phase to be rearranged into cellulose I_β phase,[16,31] which was induced on the fiber surface. It is noted that at >40 pass, the transformation rate of cellulose I_α was reduced gradually with increasing in pass when compared with that in the range from 0 to 40 pass. A previous report by Yamamoto et al.[14] proposed that cellulose nanofibers secreted by *Gluconacetobacter xylinus* were composed of I_β-rich domains as a core that were surrounded by a skin layer of cellulose I_α-rich domains. Therefore, accompanied by transformation of cellulose I_α phase into I_β in the skin proceeded by ACC treatment, the cellulose I_β phase, which is more stable crystalline phase, started to cover the surface of nanocellulose. Namely, in the obtained nanocellulose, the core of cellulose I_β surrounded by I_α was supposed to be finally surrounded by an outer skin of I_β, resulting in protecting the internal cellulose I_α from an attack of water jets in the treatment.

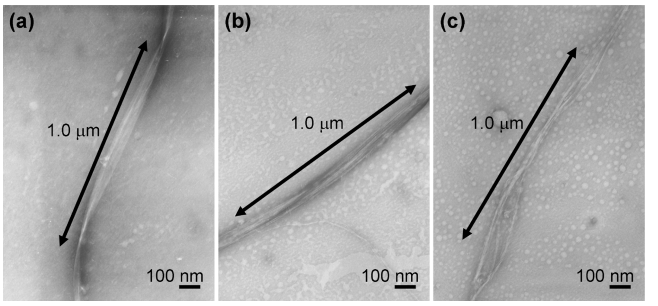

Figure 4. Releasing behaviors of the helix in a single nanocellulose by ACC treatments. All images for the fiber sample specimens with PVA were taken by TEM with (a) 0 pass, (b) 10 pass, and (c) 30 pass.

Figure 4 shows the morphology of single nanocellulose after various pass number of ACC treatment. Mixing of the nanofibers with PVA was able to prevent self-aggregation among them. Before ACC treatment, helixes were observed in the initial cellulose nanofiber. The pitch of the helix was estimated to be ca.1.0 μm, as shown in Figure 4a. This value agreed with the 0.6 to 1.0 μm pitch of the helix previously reported by Hirai et al.[32] After 10 pass of the collision, as shown in Figure 4b, the helix was started to be released. Then, nanocellulose tended to be separated into some fibrils at 30 pass, as shown in Figure 4c. At more than 30 pass, the value of width for the separated fiber was still >3.5 nm in width of a normal cellulose microfibril. Therefore, it was considered that ACC treatment was able to liberate the initial nanofibers into the individual bundles of cellulose microfibrils, not a single microfibril. As described above, the morphological changes due to ACC treatment contained releasing helix of the fiber as well as transformation of the surface crystalline phase into more stable crystalline phase.

Advantages of Nanocellulose Prepared by ACC Treatment. Here the ACC process for the microbial cellulose pellicle is compared with a more standard whiskerization procedure, such as hydrochloric acid based methods, which would easily help to stress the advantages of the ACC method that results in a cellulose nanomaterial with increased surface area but decreased length and aspect ratio. Moreover, the whiskerization process does not significantly affect the crystallinity of the cellulose. The yield of the nanoproduct in ACC treatment is almost completely 100%, which is, of course, much higher than a standard hydrochloric-acid-based whiskerization procedure. Concerning hydrochloric acid hydrolysis of the pellicle, it was reported that the ribbon-like cellulose nanofibers were fibrillated and shortened.[33] The initial nanofibers before hydrolysis had a high average degree of polymerization (DP) and narrow distribution in the size exclusion chromatogram. Upon the hydrolysis, the chromatograms shifted to a lower DP range with a broader distribution.[33] These results indicated cleavage of glucan chains as a chemical modification.

Differences between this nanocellulose and another cellulose nanofiber were marked. In our previous report,[16] wood cellulose

nanofibers were prepared from microcrystalline cellulose using ACC treatment. The length and the aspect ratio of the cellulose nanofiber were less than 1 μm and 80, respectively. In this study, nanocellulose from the microbial cellulose pellicle has a higher aspect ratio and a longer length with the intact high crystallinity, expecting cellulose fibril/whisker emulsifiers and the high reinforcement in nanocomposites, which is ideal for composite applications by considering that the high crystallinity determines the mechanical properties of the cellulose.

CONCLUSIONS

Single nanocellulose was successfully prepared from a microbial cellulose pellicle using ACC treatment. Width and length of the nanocellulose decreased with increase in the repetition times (pass) of the treatment accompanied by fibrillation on a nanoscale. Finally, width of the nanocellulose was saturated at ca. 30 nm, whereas the fiber length was longer than the molecular length (DP) of cellulose molecules in a secreted cellulose nanofiber after ACC treatment. Moreover, increasing in pass number tended to equalize the shape of the nanocellulose with less deviation of the size retaining ca. 100 of the aspect ratio. By ACC treatment, the ratio of cellulose I_α versus cellulose I_β in nanocellulose drastically changed with keeping >70% of the crystallinity. In the change of the crystalline structure of nanocellulose, our experimental results could be explained as follows: When the secreted cellulose nanofiber was separated into bundles of microfibrils by ACC treatment, the cellulose I_α phase located on the surface of the fiber was released by a shear stress because of the collision energy of water at a high speed in the treatment. Simultaneously, the motion of cellulose molecules in cellulose I_α phase on the fiber surface was encouraged to be more active to be slid, resulting in transformation into cellulose I_β phase and thereby covering cellulose I_α phase with cellulose I_β phase.

The nanocellulose exhibited high specific surface areas. Therefore, it is possible that nanocellulose has a high adsorptivity caused by the large specific surface areas. In addition, it is likely to show a more resistance against chemical reagent and more insusceptibility to enzymatic degradation caused by covering the surface with stable I_β-rich crystalline phases[34,35] when compared with the initial microbial cellulose pellicle. Furthermore, it is expected that the single nanocellulose can be applied as building blocks for functional food, fine-patterning structures, coating reagents, fillers for composites, and so on.

AUTHOR INFORMATION

Corresponding Author

*To whom correspondence should be addressed. E-mail: tekondo@agr.kyushu-u.ac.jp.

ACKNOWLEDGMENT

We thank Mr. Eiji Togawa and Ms. Yukako Hishikawa at Forestry and Forest Products Research Institute (FFPRI), Tsukuba, Japan for their kind measurements using CP/MAS ^{13}C NMR and X-ray diffraction.

REFERENCES

(1) Tokoh, C.; Takabe, K.; Fujita, M.; Saiki, H. *Cellulose* **1998**, *5*, 249–261.
(2) Helenius, G.; Bäckdahl, H.; Bodin, A.; Nannmark, U.; Gatenholm, P.; Risberg, B. *J. Biomed. Mater. Res., Part A* **2006**, *76A*, 431–438.
(3) Yamanaka, S.; Watanabe, K.; Kitamura, N. *J. Mater. Sci.* **1989**, *24*, 3141–3145.
(4) Bodin, A.; Concaro, S.; Brittberg, M.; Gatenholm, P. *J. Tissue Eng. Regener. Med.* **2007**, *1*, 406–408.
(5) Bäckdahl, H.; Esguerra, M.; Delbro, D.; Risberg, B.; Gatenholm, P. *J. Tissue Eng. Regener. Med.* **2008**, *2*, 320–330.
(6) Shah, J.; Brown, R. M., Jr. *Appl. Microbiol. Biotechnol.* **2005**, *66*, 352–355.
(7) Blaker, J. J.; Lee, K.-Y.; Li, X.; Menner, A.; Bismarck, A. *Green Chem.* **2009**, *11*, 1321–1326.
(8) Eichhorn, S. J.; Dufresne, A.; Aranguren, M.; Marcovich, N. E.; Capadona, J. R.; Rowan, S. J.; Weder, C.; Thielemans, W.; Roman, M.; Renneckar, S.; Gindl, W.; Veigel, S.; Keckes, J.; Yano, H.; Abe, K.; Nogi, M.; Nakagaito, A. N.; Mangalam, A.; Simonsen, J.; Benight, A. S.; Bismarck, A.; Berglund, L. A.; Peijs, T. *J. Mater. Sci.* **2010**, *45*, 1–33.
(9) Lin, K.-W.; Lin, H.-Y. *J. Food Sci.* **2004**, *69*, SNQ107–111.
(10) Klemm, D.; Schumann, D.; Kramer, F.; Hessler, N.; Hornung, M.; Schmauder, H. -P.; Marsch, S. *Adv. Polym. Sci.* **2006**, *205*, 49–96.
(11) Shibazaki, H.; Kuga, S.; Okano, T. *Cellulose* **1997**, *4*, 75–87.
(12) Czaja, W.; Romanovicz, D.; Brown, R. M., Jr. *Cellulose* **2004**, *11*, 403–411.
(13) Atalla, R. H.; Vanderhart, D. L. *Science* **1984**, *223*, 283–285.
(14) Yamamoto, H.; Horii, F.; Hirai, A. *Cellulose* **1996**, *3*, 229–242.
(15) Kondo, T.; Morita, M.; Hayakawa, K.; Onda, Y. U.S. Patent 7,357,339, 2005.
(16) Kondo, T.; Kose, R.; Naito, H.; Takada, A.; Kasai, W. *Colloid Polym. Sci.* **2010** submitted.
(17) Hestrin, S.; Schramm, M. *Biochem. J.* **1954**, *58*, 345–352.
(18) Kataoka, Y.; Kondo, T. *Int. J. Biol. Macromol.* **1999**, *24*, 37–41.
(19) Chen, Y.; Stipanovic, A. J.; Winter, W. T.; Wilson, D. B.; Kim, Y.-J. *Cellulose* **2007**, *14*, 283–293.
(20) Yamamoto, H.; Horii, F. *Macromolecules* **1993**, *26*, 1313–1317.
(21) Brunauer, S.; Emmett, P. H.; Teller, E. *J. Am. Chem. Soc.* **1938**, *60*, 309–319.
(22) TAPPI Standard T230 su-66.
(23) Vink, H. In *Cellulose and Cellulose Derivatives Part IV*; Bikales, N. M., Segal, L., Eds.; John Wiley & Sons: New York, NY, 1971; p 469.
(24) Ardizzone, S.; Dioguardi, F. S.; Mussini, T.; Mussini, P. R.; Rondinini, S.; Vercelli, B.; Vertova, A. *Cellulose* **1999**, *6*, 57–69.
(25) Sanchavanakit, N.; Sangrungraungroj, W.; Kaomongkolgit, R.; Banaprasert, T.; Pavasant, P.; Phisalaphong, M. *Biotechnol. Prog.* **2006**, *22*, 1194–1199.
(26) Haigler, C. H.; White, A. R.; Brown, R. M., Jr.; Cooper, K. M. *J. Cell Biol.* **1982**, *94*, 64–69.
(27) Bondeson, D.; Mathew, A.; Oksman, K. *Cellulose* **2006**, *13*, 171–180.
(28) Marrinan, H. J.; Mann, J. *J. Polym. Sci.* **1956**, *XXI*, 301–311.
(29) Sugiyama, J.; Persson, J.; Chanzy, H. *Macromolecules* **1991**, *24*, 2461–2466.
(30) Kataoka, Y.; Kondo, T. *Macromolecules* **1996**, *29*, 6356–6358.
(31) Wada, M.; Kondo, T.; Okano, T. *Polym. J.* **2003**, *35*, 155–159.
(32) Hirai, A.; Tsuji, M.; Horii, F. *Sen'i Gakkaishi* **1998**, *54*, 506–510.
(33) Shibazaki, H.; Kuga, S.; Onabe, F.; Brown, R. M., Jr. *Polymer* **1995**, *36*, 4971–4976.
(34) Hayashi, N.; Sugiyama, J.; Okano, T.; Ishihara, M. *Carbohydr. Res.* **1998**, *305*, 109–116.
(35) Hayashi, N.; Kondo, T.; Ishihara, M. *Carbohydr. Polym.* **2005**, *61*, 191–197.